

# A novel oral rabies vaccine enhances the immunogenicity through increasing dendritic cells activation and germinal center formation by expressing U-OMP19 in a mouse model

Jianqing Zhao<sup>a,b,\*</sup>, Yijing Zhang<sup>b,\*</sup>, Yixi Chen<sup>a,b</sup>, Juntao Zhang<sup>b</sup>, Jie Pei<sup>a,b</sup>, Min Cui<sup>a,b</sup>, Zhen F. Fu<sup>a,b</sup>,  
Ling Zhao<sup>a,b</sup> and Ming Zhou<sup>b</sup>

<sup>a</sup>State Key Laboratory of Agricultural Microbiology, Huazhong Agricultural University, Wuhan, People's Republic of China; <sup>b</sup>Key Laboratory of Preventive Veterinary Medicine, College of Veterinary Medicine, Huazhong Agricultural University, Wuhan, People's Republic of China

## ABSTRACT

Rabies remains a public health threat in most parts of the world. Dogs, especially stray dogs, are the main sources of rabies transmission in developing countries, while wild animals are primarily responsible for the spread of rabies in developed countries and play an emerging role in rabies transmission in developing countries. Oral vaccination is the most practical method for rabies control in these animals, and the greatest challenge for oral vaccination is the hostile environment and large quantity of proteases in the gastrointestinal tract. In the present study, a promising adjuvant with potential protease inhibitory activity, unlipidated outer membrane protein 19 (U-OMP19), was inserted into the genome of the recombinant rabies virus (rRABV) strain LBNSE, designated LBNSE-U-OMP19, and the immunogenicity of LBNSE-U-OMP19 was investigated. LBNSE-U-OMP19 could potentially protect viral glycoprotein from digestion by gastrointestinal fluids *in vitro*. The expression of U-OMP19 attenuated viral pathogenicity by restricting viral replication in the central nervous system (CNS) and repressing the production of inflammatory chemokines and cytokines. After oral vaccination, LBNSE-U-OMP19 recruited dendritic cells (DCs), follicular helper T (T<sub>FH</sub>) cells and germinal center (GC) B cells, promoted the formation of GCs, and increased the population of plasma cells in immunized mice, resulting in higher levels of RABV-neutralizing antibodies and better protection in mice immunized with LBNSE-U-OMP19 than in those immunized with the parent virus LBNSE. Together, our data suggest that LBNSE-U-OMP19 is a promising candidate for oral rabies vaccines.

**ARTICLE HISTORY** Received 9 December 2020; Revised 14 April 2021; Accepted 23 April 2021

**KEYWORDS** Rabies; oral rabies vaccine; U-OMP19; dendritic cells; germinal center; potential gastrointestinal proteases resistance

## Introduction


Rabies, as an ancient zoonotic disease, is caused by rabies virus (RABV). It still poses a public threat worldwide, especially in those developing countries with poor infrastructure and medical conditions [1,2]. The main source for rabies transmission in developing countries is dogs, especially free-roaming dogs [3,4], which are responsible for up to 99% of all rabies transmissions to humans. It has been reported that vaccination of over 70% of the canine population efficiently reduce rabies transmission and human cases [5,6]. In developed countries, bats and other wild animals are mainly responsible for rabies [7]. Recently, rabies in other species of wildlife, such as Chinese ferret badgers, greater tube-nosed bats, and raccoon dogs, has been increasingly reported, suggesting that wild animals can also serve as rabies reservoirs and play an emerging role in the transmission of rabies to humans and livestock [8–10]. Therefore, increasing

rabies vaccination of free roaming dogs and wild animals could be crucial for rabies control worldwide, and the most practical method of rabies vaccination for these animals is oral vaccination.

Currently, two oral rabies vaccines are widely used in Europe for wildlife and are recommended for dog vaccination by the World Health Organization (WHO) [11]. One is SAG-2, which is a mutated form of Street-Alabama-Dufferin strain (SAD) with two nucleotide mutations at its glycoprotein (G) codon 333 [12]; however, the virus-neutralizing antibody (VNA) titres induced by SAG-2 are generally low in dogs after oral vaccination, and not all vaccinated dogs develop detectable VNA titres [13–15]. The other vaccine is a recombinant vaccinia virus expressing RABV glycoprotein (VRG), which is a recombinant vaccinia virus expressing RABV G protein [16]. VRG has been successfully used for rabies control of foxes in Europe and rabies control

**CONTACT** Ming Zhou  mikchail@163.com; Ling Zhao  zling604@yahoo.com

\*Equal contribution.

 Supplemental data for this article can be accessed <https://doi.org/10.1080/22221751.2021.1923341>.

© 2021 The Author(s). Published by Informa UK Limited, trading as Taylor & Francis Group.

This is an Open Access article distributed under the terms of the Creative Commons Attribution-NonCommercial License (<http://creativecommons.org/licenses/by-nc/4.0/>), which permits unrestricted non-commercial use, distribution, and reproduction in any medium, provided the original work is properly cited.

of coyotes and raccoons in the United States [17–19]. Nevertheless, two humans experienced intense skin inflammation and systemic vaccinia infection after VRG exposure, suggesting potential safety issues for humans who are in close contact with vaccinated dogs [20]. Previous studies have demonstrated that immune responses after oral rabies vaccination mainly develop in the oral cavity rather than the gut due to the acidic conditions of the stomach and intestine [21–23]. Therefore, it would be a promising strategy to develop an oral rabies vaccine could activate the immune responses in both oral cavity and gastrointestinal tract.

Unlipidated outer membrane protein 19 (U-OMP19) is a protease inhibitor from *Brucella spp.* that has been used as an oral adjuvant to activate the immune responses in gut as described previously [24]. It was demonstrated that U-OMP19 could not only weaken the digestion of antigens by pancreatic and brush border proteases, but also stimulate intestinal epithelial cells to accelerate the intake of antigens and reduce degradation in the process of presentation. Simultaneously, it can inhibit cellular lysosomes, help complete antigens to be further transferred to the antigen presenting cells (APC) in the lamina propria and enhance specific immunity mediated by T cells eventually. Combined vaccination of U-OMP19 with antigens derived from enteric pathogens induced a better host immune response than vaccination with the antigens alone [25,26]. Therefore, in the present study, a novel oral rabies vaccine that a recombinant RABV expressing U-OMP19 was constructed based on the parent virus LBNSE. LBNSE is a SAG-2 equivalent that contains two mutations at amino acids 333 and 194 of the G protein that was demonstrated to be avirulent in a previous study [27]. It was found that a recombinant RABV (rRABV) expressing U-OMP19 could improve VNA production and protection after oral immunization by activating the dendritic cell (DC)-follicular helper T ( $T_{FH}$ ) cell-germinal center (GC) B cell-plasma cell (PC) axis as well as generating more GCs in both cervical lymph nodes (CLNs) and mesenteric lymph nodes (MLNs) in a mouse model, suggesting that LBNSE-U-OMP19 is a novel oral rabies vaccine candidate.

## Materials and methods

### Viruses, Cells, Antibodies, Reagents and Animals

The RABV strain LBNSE is a form of the SAD-B19 with mutations at amino acids 194 and 333 in the G protein [27]. The pathogenic RABV strain CVS-24 was propagated in the brains of suckling ICR mice. The BSR cell lines is derived from the BHK-21 cell line, and mouse neuroblastoma (NA) cells were

cultured in Dulbecco's modified Eagle's medium (DMEM) (Gibco) containing 10% FBS (Gibco). Fluorescein isothiocyanate (FITC)-conjugated antibodies against the RABV N protein were purchased from Fujirebio Diagnostics, Inc. The (HRP)-conjugated goat anti-mouse IgA antibody was purchased from Proteintech. The HRP-conjugated goat anti-mouse IgM antibody was purchased from Bioss. The antibodies used to label cells for flow cytometry were purchased from BioLegend, including FITC-conjugated anti-mouse CD11c (clone N418), FITC-conjugated anti-mouse CD4 (clone GK1.5), FITC-conjugated anti-mouse/human CD45R/B220 (clone RA3-6B2), PE-conjugated anti-mouse CD86 (clone GL-1), PE-conjugated anti-mouse CD279 (PD-1) (clone RMP1-30), PE/Cy7-conjugated anti-mouse I-A/I-E (MHC-II) (clone M5/114.15.2), and APC-conjugated anti-mouse CD185 (CXCR5) (clone L138D7), and other antibodies, including Alexa Fluor 647-conjugated anti-mouse/human GL7 (clone GL7), were also purchased from BioLegend, while PE-conjugated anti-mouse CD95 (APO-1/Fas) (clone 15A7) was purchased from eBioscience. The antibodies used to fluorescently stain GCs in lymph nodes were purchased from BioLegend, including biotin-labelled anti-human/mouse GL7, Alexa Fluor 647-conjugated anti-mouse/human CD45R/B220 and Alexa Fluor 488-conjugated goat anti-mouse IgG, and the Alexa Fluor 594-conjugated streptavidin that was used to label GL7 was purchased from eBioscience. SuperFect transfection reagent was purchased from Qiagen. RIPA buffer and an enhanced chemiluminescence (ECL) detection kit were purchased from Beyotime. PVDF membranes were purchased from Bio-Rad. Reference serum was obtained from the National Institute for Biological Standards and Control. TRIzol was purchased from Invitrogen. HiScript III 1st Strand cDNA Synthesis Kit and ChamQ SYBR qPCR Master Mix were purchased from Vazyme. The staining buffer used for FACS was purchased from BD Biosciences. Pepsin and trypsin were purchased from Sangon Biotech and Gibco, respectively. ICR mice were purchased from the Chinese Center for Disease Control and Prevention of Hubei Province, China.

### Construction and rescue of rRABV expressing U-OMP19

The vector containing LBNSE was constructed as previously described [28]. The *BsiWI* and *NheI* restriction sites were introduced between the G and RNA-dependent RNA-polymerase (L) genes. The original U-OMP19 sequence was synthesized by Genescript. Briefly, the U-OMP19 gene was cloned and inserted into the vector pLBNSE to generate pLBNSE-U-OMP19, and the primers for amplifying the U-OMP19 gene are listed in Table 1. For virus rescue,

the constructed infectious clone pLBNSE-U-OMP19 and four helper plasmids expressing the Nucleoprotein (N), Phosphoprotein (P), G and L proteins were cotransfected into BSR cells using the SuperFect transfection reagent according to the manufacturer's instructions [28,29]. After transfection, the BSR cells were washed with DMEM for three times to remove the residual transfection reagents and plasmids, and fresh culture medium were then added. After four days of incubation, the culture medium was harvested and examined for the presence of rescued virus with FITC-conjugated anti-RABV N antibodies.

### Virus titration

Virus titres were detected with the direct fluorescent antibody assay as described previously [30]. Briefly, a serial 10-fold dilution of the virus was inoculated into BSR cells in 96-well microplates in quadruplicate, and the cells were incubated at 37°C for 48 h. After incubation, the medium was discarded, and the cells were fixed with 80% ice-cold acetone and stained with FITC-conjugated RABV N protein-specific antibodies for 1 h. Antigen-positive foci were counted under a fluorescence microscope (Zeiss), and the virus titre was calculated as the fluorescent focus units per millilitre (FFU/mL).

### Specific antibody detection using ELISA

ELISA plates were coated with 500 ng/well of LBNSE diluted in coating buffer overnight at 4°C. Then, plates were washed three times in PBST and blocked in PBS with 5% skim milk at 37°C for 2 h. To detect RABV-specific IgM, blood samples were collected from orally immunized mice weekly for two weeks, and the sera were separated and incubated in plates coated with LBNSE at 37°C for 2 h. After the plates were washed three times with PBST, HRP-conjugated goat anti-mouse IgM was added to the plates at 37°C for 1 h. All plates were washed three times with PBST, TMB substrate buffer was added to the plates for 15 min in the dark, and 2 M H<sub>2</sub>SO<sub>4</sub> was added to stop the reaction. The optical density was read at 450 nm by using a SpectraMax 190 spectrophotometer (Molecular Devices).

### Western blotting

Infected cells were trypsinized and washed twice with ice-cold PBS. Proteins were extracted with RIPA buffer. After centrifugation, the supernatants were separated by 12% SDS-PAGE and transferred to PVDF membranes. After being blocked with 5% skimmed milk for 3 h, the membrane was incubated with primary antibodies overnight and washed twice with TBST. The HRP-conjugated secondary antibody

was added, and the samples were incubated for 1 h at room temperature. Signals were detected with an ECL detection kit.

### Gastrointestinal fluid incubation assay

Gastric fluids and intestinal fluids were formulated according to the guidelines of Pharmacopoeia. Briefly, to construct simulated gastric fluids, 234 mL of concentrated hydrochloric acid was diluted to 1L, and 16.4 mL of the above solution was taken and diluted with distilled water to 800 mL. Finally, 10 g of pepsin was added and dissolved, and then distilled water was added to make the total volume up to 1L. For simulated intestine fluids, 6.8 g of potassium dihydrogen phosphate was dissolved with 500 ml of distilled water and the pH value was adjusted to 6.8 with 0.1 mol/l sodium hydroxide solution. Finally, 10 g of trypsin was dissolved and mixed with the above solution, and the volume of solution was made to 1000 ml with distilled water. Before the incubation assay, the enzyme activity of the simulated fluids including gastric fluids and intestinal fluids were detected individually by the Enzyme Activity Assay Kit purchased from Solarbio. Equal titres of LBNSE and LBNSE-U-OMP19 were incubated with these different fluids in the same volumes for 1 or 2 h. The gastric supernatants were neutralized with sodium bicarbonate. Parts of the supernatants were used to measure virus titres as described above. The others were mixed with quadruple volume of cold acetone and incubated overnight. After centrifugation, RIPA buffer was added to dissolve the pellets. Proteins were detected by western blotting according to the previous study [31].

### Pathogenicity studies

To confirm whether the expression of U-OMP19 could affect the pathogenicity of RABV *in vivo*, six-week-old female ICR mice and five-day-old suckling ICR mice were inoculated via the intracranial (i.c.) route with  $3 \times 10^6$  and 100 FFU of rRABVs, respectively, and the same volume of DMEM was inoculated as a negative control. The body weight change and survival rates were recorded daily for three weeks, and the levels of viral genomic RNA and mRNA of RABV N protein, U-OMP19, and inflammatory cytokines such as IL-1 $\beta$ , TNF- $\alpha$ , and IL-6 were determined by qRT-PCR assay.

### qRT-PCR assay

To measure the levels of mRNA transcription and virus replication in mouse samples, genomic RNA and specific RABV N protein mRNA were measured in mouse brains infected with LBNSE, LBNSE-U-

OMP19 and DMEM. Total RNA was extracted by TRIzol and reverse transcribed with a HiScript III 1st Strand cDNA Synthesis Kit. All samples were detected with ChamQ SYBR qPCR Master Mix, and the primers are listed in Table 1. Standards were derived from the RABV N gene. The curves were constructed using cycle threshold (CT) values that were obtained using dilutions of the standards. The mRNA and genomic RNA copy numbers in each sample were normalized to the respective copy numbers that were derived from the standard curve. The following programme was used: 95°C for 2 min for one cycle followed by 40 cycles at 95°C for 5 s and 60°C for 30 s. The specific primers are listed in Table 1.

### **Nest PCR assay**

In order to investigate whether the vaccine virus could replicate in the oral cavity after oral immunization, the buccal mucosa, CLNs and tongues of the immunized mice were collected and the total RNA were extracted to detect the viral RNA by primary RT-PCR and nest PCR as previously described [13,32]. The primers for RT-PCR and nest PCR were listed in supplementary Table 1.

### **Direct fluorescent antibody test (DFAT)**

To test whether the sacrificed suckling mice died of RABV infection, the brain samples of dead suckling mice were collected and subjected to DFAT. Briefly, the small pieces of the selected brain sections were grouped on a wooden applicator stick, and an impression smear was made directly onto the slide. Impression smear preparations of the brain samples were placed in a Coplin jar containing 80% cold acetone within the freezer for 30 min. The slides were air-dried and incubated with FITC-conjugated antibodies against the RABV N protein for 45 min at 37°C in a humid chamber. After incubation, the slides were washed with PBST for three times, air-dried and then visualized under a fluorescent microscope. Bright apple-green or yellow-green inclusions indicate RABV-positive.

### **Oral vaccination test**

To assess the protection against rabies induced by the recombinant vaccine, three groups of six-week-old female ICR mice ( $n = 20$ ) were orally immunized with  $10^7$  FFU of LBNSE or LBNSE-U-OMP19 or mock immunized with the same volume of DMEM. At four weeks post immunization (wpi), mice were challenged with 50 LD<sub>50</sub> of CVS-24 via the i.c. route and monitored daily for 21 days, and the body weight changes and survival rates were recorded accordingly.

To assess the efficacy of U-OMP19 as an adjuvant for inactivated oral rabies vaccines,  $10^7$  FFU of LBNSE was UV inactivated and mixed with 150 µg of U-OMP19. Three groups ( $n = 10$ ) of six-week-old female ICR mice were orally immunized with  $10^7$  FFU of inactivated LBNSE and U-OMP19 or  $10^7$  FFU of inactivated LBNSE or mock immunized with the same volume of DMEM. Blood samples were collected weekly from 2 to 5 wpi. At 5 wpi, mice were challenged with 50 LD<sub>50</sub> of CVS-24 via the i.c. route and monitored daily for 21 days, and the body weight changes and survival rates were recorded accordingly.

### **VNA test**

VNA titres were calculated using the fluorescent antibody virus neutralization (FAVN) test as previously described [33]. Fifty microlitres of serial three-fold dilutions of mouse serum collected from peripheral blood and standard serum were prepared in 96-well microplates with 100 µL of DMEM. The tests were detected in quadruplicate. A 50 µL suspension containing 100 FFU of a rabies challenge virus, CVS-11, was added to each well. After incubation at 37°C for 1 h,  $2 \times 10^4$  BSR cells were added to each well and incubated at 37°C for 48 h. After incubation, the culture medium was discarded, and the cells were fixed with 80% ice-cold acetone for 30 min and stained with FITC-conjugated antibodies against the RABV N protein. The results were observed by an Olympus IX51 fluorescence microscope and calculated in IU/mL by comparison to reference serum.

### **Histology and immunofluorescence assays**

CLNs and MLNs of orally immunized mice were collected and fixed with 4% paraformaldehyde for 48 h. Then, the tissues were dehydrated with 30% sucrose and cut into 30 µm-thick sections. Sections were fluorescently stained with Alexa Fluor 647-conjugated anti-mouse/human CD45R/B220, Alexa Fluor 488-conjugated goat anti-mouse IgG, and biotin-labelled anti-human/mouse GL7 followed by staining with Alexa Fluor 594-conjugated streptavidin [34]. Images were captured under an Olympus IX51 fluorescence microscope.

### **FACS analysis**

Groups of six-week-old female ICR mice were orally immunized with  $10^7$  FFU of LBNSE or rLBNSE-U-OMP19 or mock immunized with DMEM. CLNs, MLNs and bone marrow were collected at 7 or 14 dpi. Single-cell suspensions ( $10^5$  cells/sample) were incubated in staining buffer with fluorescence-conjugated antibodies for 30 min at 4°C in the dark. Cells were washed twice with PBS containing 0.2%

BSA and fixed in 4% paraformaldehyde for 30 min. Data collection and analysis were performed using a BD LSR-II flow cytometer, BD FACS-Diva software, and FlowJo software (TreeStar).

### Statistical analysis

All data were analysed using GraphPad Prism 8. To determine the percent survival, Kaplan-Meier survival curves were analysed using the log-rank test. For the other data, an unpaired two-tailed t-test was used to determine whether differences were statistically significant. Data are representative of two independent experiments. For all results, the following notations are used to indicate significant differences between groups: \* $p < 0.05$ , \*\* $p < 0.01$ ; \*\*\* $p < 0.001$ ; and \*\*\*\* $p < 0.0001$ .

## Results

### Construction of an rRABV expressing U-OMP19 and evaluation of its gastrointestinal protease resistance *in vitro*

As shown in Figure 1(A), the U-OMP19 gene was cloned and inserted between the G and L genes within the genome of the RABV strain LBNSE, which is a form of the oral vaccine strain SAD-B19 with two mutations at amino acids 194 and 333 of the G protein. The rRABV expressing U-OMP19 was then rescued as shown in Figure S6A and designated as LBNSE-U-OMP19. The growth curves of LBNSE-U-OMP19 in BSR and NA cells were generated and compared with that of the parent virus LBNSE. As shown in Figure 1(B) and (C), the growth curves of LBNSE-U-OMP19 in BSR and NA cells were similar to that of LBNSE, suggesting that the insertion of the U-OMP19 gene into the LBNSE genome did not affect viral replication. Furthermore, the expression of U-OMP19 was then detected by western blotting assay as shown in Figure 1(D), and U-OMP19 was well expressed in a dose-dependent manner by the BSR cells infected with LBNSE-U-OMP19 in both cell lysates and culture supernatants.

As U-OMP19 has been demonstrated to be a protease inhibitor [25], the potential of LBNSE-U-OMP19 and LBNSE to resist stomach and intestine proteases was compared by detecting the levels of G protein, the only exposed and immunogenic protein of RABV, and N protein using western blotting assays after incubation with simulated stomach or intestine fluid. The enzyme activity of simulated gastric fluid and intestinal fluid were verified as shown in Figure S3A and S3B respectively. As shown in Figure 1(E), after incubation with simulated stomach fluid for 1 h, more G and N proteins

of LBNSE were digested than those of LBNSE-U-OMP19 according to the exhibited bands, especially after 2 h of incubation, at which point almost all the G and N proteins of LBNSE were digested, while clear and thick bands of the G and N proteins of LBNSE-U-OMP19 were still observed. Similar results were observed after incubation with simulated intestine fluid, as shown in Figure 1(F). Moreover, to determine whether the expression of U-OMP19 could potentially protect viral replication ability, the viral titres of rRABVs after incubation with stomach or intestine protease solution were also measured. Nevertheless, no detectable or dramatically decreased virus titres were observed after incubation with simulated stomach or intestine fluids for either LBNSE or LBNSE-U-OMP19 respectively (data not shown), indicating that expressing U-OMP19 could not effectively protect the viral replication ability. These data indicate that the expression of U-OMP19 by LBNSE-U-OMP19 has the potential to reduce the digestion of viral proteins by simulated stomach and intestine fluids *in vitro*, and whether the potential effect still hold true *in vivo* needs further investigations.

### Expression of U-OMP19 attenuates RABV pathogenicity *in vivo*

The safety of vaccine strains is an important assessment for live vaccines; therefore, the pathogenicity of LBNSE-U-OMP19 was assessed in a mouse model by direct injection of the virus into the brains of mice through the i.c. route. Neither death nor clinical neurological symptoms were observed in mice infected with LBNSE or LBNSE-U-OMP19 during the observed period. For body weight change, mice injected with LBNSE were significantly decreased from 3 to 10 days post infection (dpi) compared with those of mice injected with LBNSE-U-OMP19 or those of mice mock injected with DMEM, as shown in Figure 2(A). Moreover, as shown in Figure 2 (B) and (C), the levels of viral RNA and rRABV N gene mRNA were measured by qRT-PCR in the brain samples of infected mice at 3 and 6 dpi, and significantly higher levels of viral RNA and mRNA were detected in the brains of LBNSE-infected mice than in those of LBNSE-U-OMP19-infected mice. Meanwhile, a significantly higher level of U-OMP19 mRNA was detected in LBNSE-U-OMP19-infected mice at 3 dpi, as shown in Figure 2(D). The above data indicate that LBNSE-U-OMP19 had decreased viral pathogenicity in mice because of expression of U-OMP19. To further explore the possible reasons for this attenuation, inflammatory cytokine levels were determined by qRT-PCR, and the mRNA levels of IL-6, TNF- $\alpha$ , and IL-1 $\beta$  were significantly decreased in the brains of mice infected with

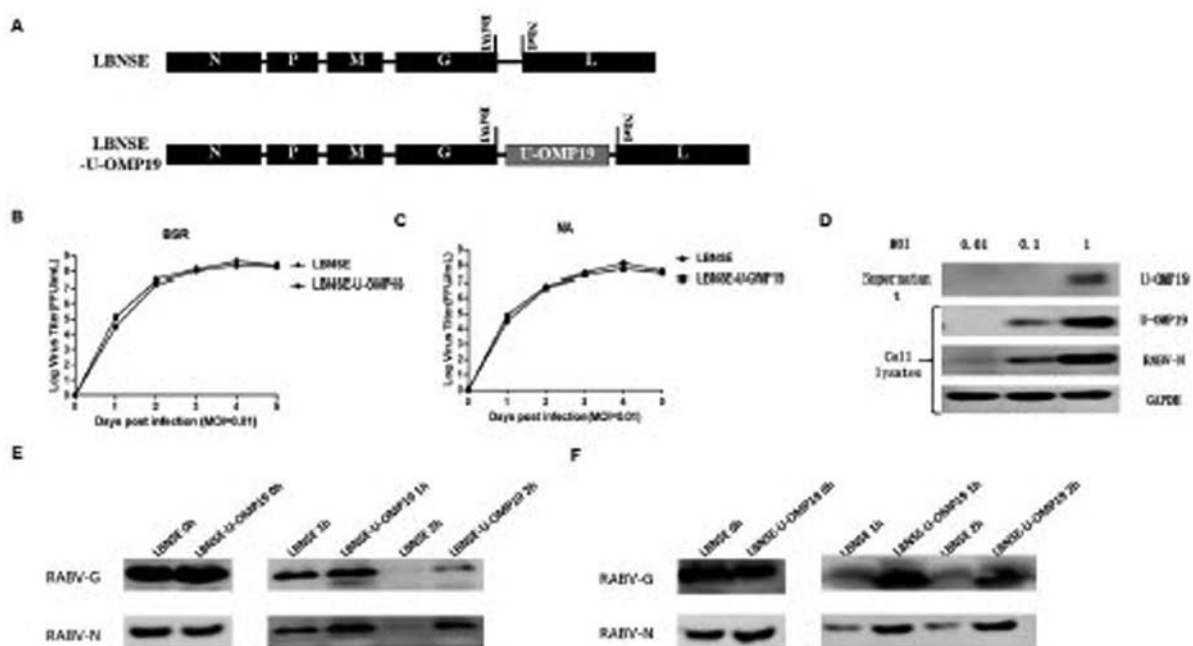


**Figure 1** . Strategy for the construction of rRABV expressing U-OMP19 and the evaluation of its gastrointestinal protease resistance *in vitro*. (A) Schematic diagram for the construction of LBNSSE-U-OMP19. The parent vector pLBNSSE was constructed based on the SAD-B19 strain by deleting the pseudogene between the G and L genes where BsiwI and NheI restriction enzyme sites were introduced. N, P, M, G and L represent the nucleoprotein, phosphoprotein, matrix, glycoprotein, and polymerase genes of RABV, respectively. Multistep virus growth curves were determined with BSR cells (B) and NA cells (C). Cells were infected with either LBNSSE or LBNSSE-U-OMP19 at a multiplicity of infection (MOI) of 0.01. Culture supernatants were collected at 1, 2, 3, 4 and 5 dpi for viral titration. The virus growth curves were drawn according to the viral titres measured at each time point, and data are presented as the mean  $\pm$  SEM ( $n = 3$ ). (D) Expression of U-OMP19 was detected in infected BSR cells by western blotting. BSR cells were infected with rRABVs at different MOIs (1, 0.1 and 0.01), and cells were collected at 48 post infection. The expression of U-OMP19, RABV N and GAPDH was detected in cell lysates by western blotting, and the expression of U-OMP19 was detected in culture supernatants as well. The degradation of RABV G and N proteins after 1 h or 2 h of incubation with artificial fluids, including gastric fluids (E) and intestinal fluids (F), was detected by western blotting assay. The data are representative of results from two independent experiments. (\* $p < 0.05$ ; \*\* $p < 0.01$ ).

LBNSSE-U-OMP19 compared with the respective levels in the brains of mice infected with LBNSSE, as shown in Figure 2(E)–(G), indicating that the decreased pathogenicity of LBNSSE-U-OMP19 in mice was most likely due to the reduction in central nervous system (CNS) inflammation caused by the expression of U-OMP19. Furthermore, to examine whether the expression of U-OMP19 can also decrease the pathogenicity of RABV in immunocompromised mice, groups of five-day-old ICR mice were inoculated with 100 FFU of different rRABVs via the i.c. route, and the clinical signs of rabies and survival rates were observed and recorded. As shown in Figure 2(H), all the suckling mice injected with LBNSSE succumbed to infection from 6 to 10 dpi, while 43.75% of the suckling mice injected with LBNSSE-U-OMP19 did not develop any clinical signs of rabies and survived. To confirm that the suckling mice succumbed to rabies, the brains of dead suckling mice were harvested and analysed for RABV infection with the direct fluorescent antibody test (DFAT), as shown in Figure S2. Together, the results demonstrate that the expression of U-OMP19 attenuates RABV pathogenicity in mice.

### Recruitment and activation of DCs in mice orally immunized with LBNSSE-U-OMP19

Our previous studies have demonstrated that recruitment and activation of DCs can enhance the immunogenicity of oral rabies vaccines. Therefore, the mice were orally immunized with a needleless syringe with  $10^7$  FFU of LBNSSE-U-OMP19 or LBNSSE or mock immunized with DMEM, and the CLNs and MLNs of immunized mice were collected at the indicated time points and subjected to FACS analysis. The gating strategy and representative flow cytometric plots for activated DCs ( $CD11c^+CD80^+$  or  $CD11c^+CD86^+$ ) are as shown in Figure 3(A) and (B), respectively. As expected, the numbers of activated DCs detected in both the CLNs and MLNs of mice immunized with LBNSSE-U-OMP19 were significantly higher than those detected in the CLNs and MLNs of mice immunized with LBNSSE at 7 dpi, as shown in Figure 3(C) and (D). In addition, significant more activated DCs were detected in CLN of LBNSSE immunized mice than those of mock immunized mice at both 7 and 14 days post immunization. In contrast, no significant difference on DCs activation in MLN

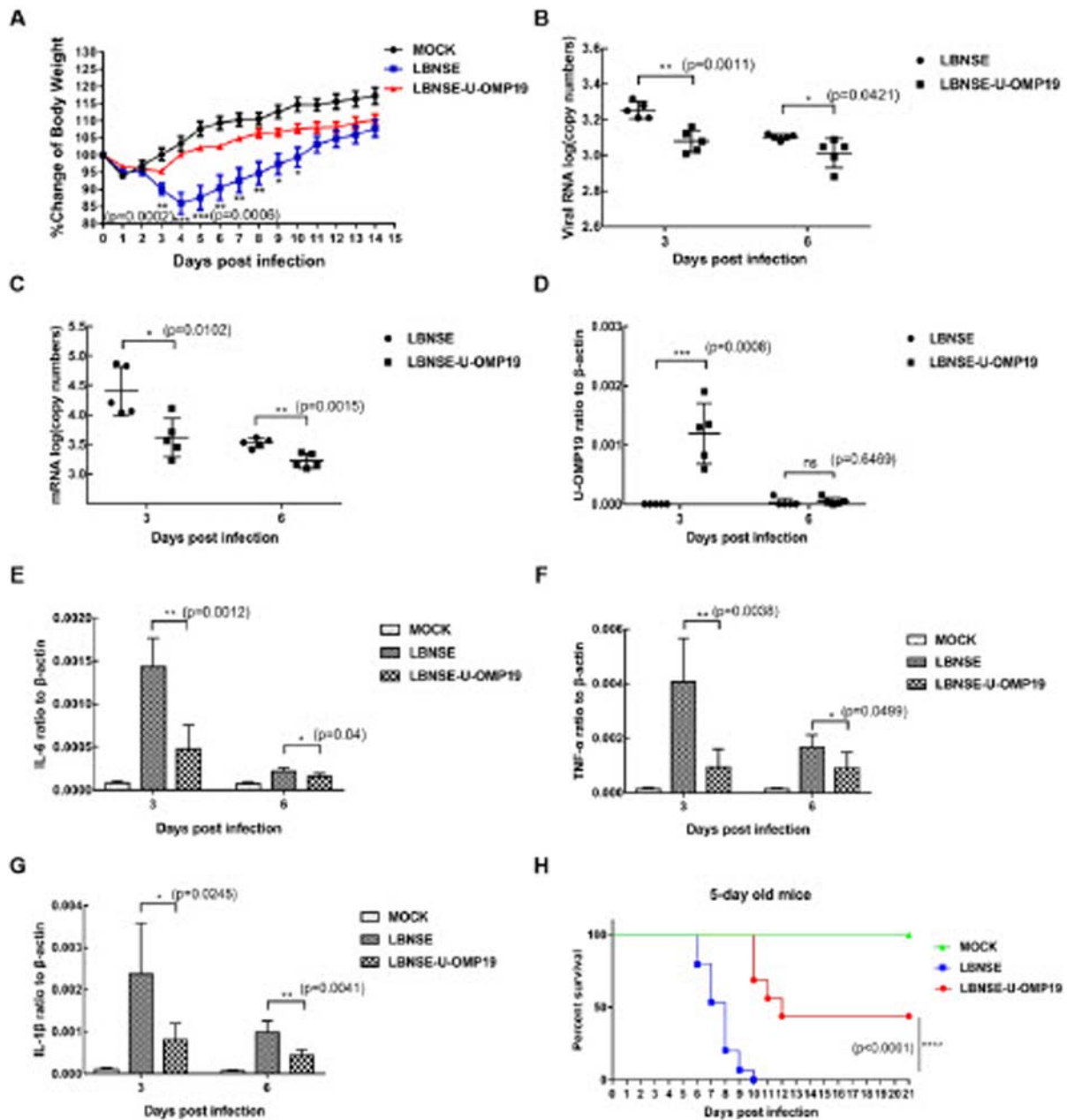


**Figure 2.** Expression of U-OMP19 attenuates RABV pathogenicity *in vivo*. Groups of six-week-old female ICR mice ( $n = 10$ ) were inoculated via the i.c. route with  $3 \times 10^6$  FFU of LBNSE or LBNSE-U-OMP19 or mock injected with DMEM. Body weight losses were monitored for 14 days, and the body weight change curves are depicted (A). Furthermore, groups of 6-week-old female ICR ( $n = 5$ ) were infected via the i.c. route with  $3 \times 10^6$  FFU of LBNSE or LBNSE-U-OMP19, and the levels of viral genomic RNA (B) and the mRNA levels of RABV N (C), U-OMP19 (D), IL-1 $\beta$  (E), TNF- $\alpha$  (F) and IL-6 (G) were quantified by qRT-PCR. To evaluate the pathogenicity of rRABVs in suckling mice, litters of 5-day-old ICR mice ( $n = 15$ ) were infected via the i.c. route with 100 FFU of LBNSE or LBNSE-U-OMP19 or mock infected with DMEM, and survival rates were monitored daily for 21 days (H). The error bars represent the mean  $\pm$  SEM ( $n = 5$ ), and the data are representative of the results of two independent experiments. ( $*p < 0.05$ ;  $**p < 0.01$ ;  $***p < 0.001$ ;  $****p < 0.0001$ ).

were observed except that only significantly more CD11c<sup>+</sup> CD86<sup>+</sup> DCs ( $p = 0.019$ ) were observed in MLN of LBNSE immunized mice than mock immunized mice at seven days post immunization as shown in Figure 3(E) and (F), indicating that the lack of activation in MLNs most likely depends on protease digestion by gastrointestinal proteases. These data suggest that mice orally immunized with LBNSE-U-OMP19 have enhanced recruitment and/or activation of DCs in both CLNs and MLNs.

### Expression of U-OMP19 enhances the recruitment of T<sub>FH</sub> cells and the generation of GCs in orally immunized mice

After the capture and presentation of antigens by antigen-presenting cells (APCs), such as DCs, activated DCs interact with CD4<sup>+</sup> naïve T cells, which then differentiate into different subtypes, including T<sub>FH</sub> cells. T<sub>FH</sub> cells play an important role in GC formation and are essential for high-affinity antibody production

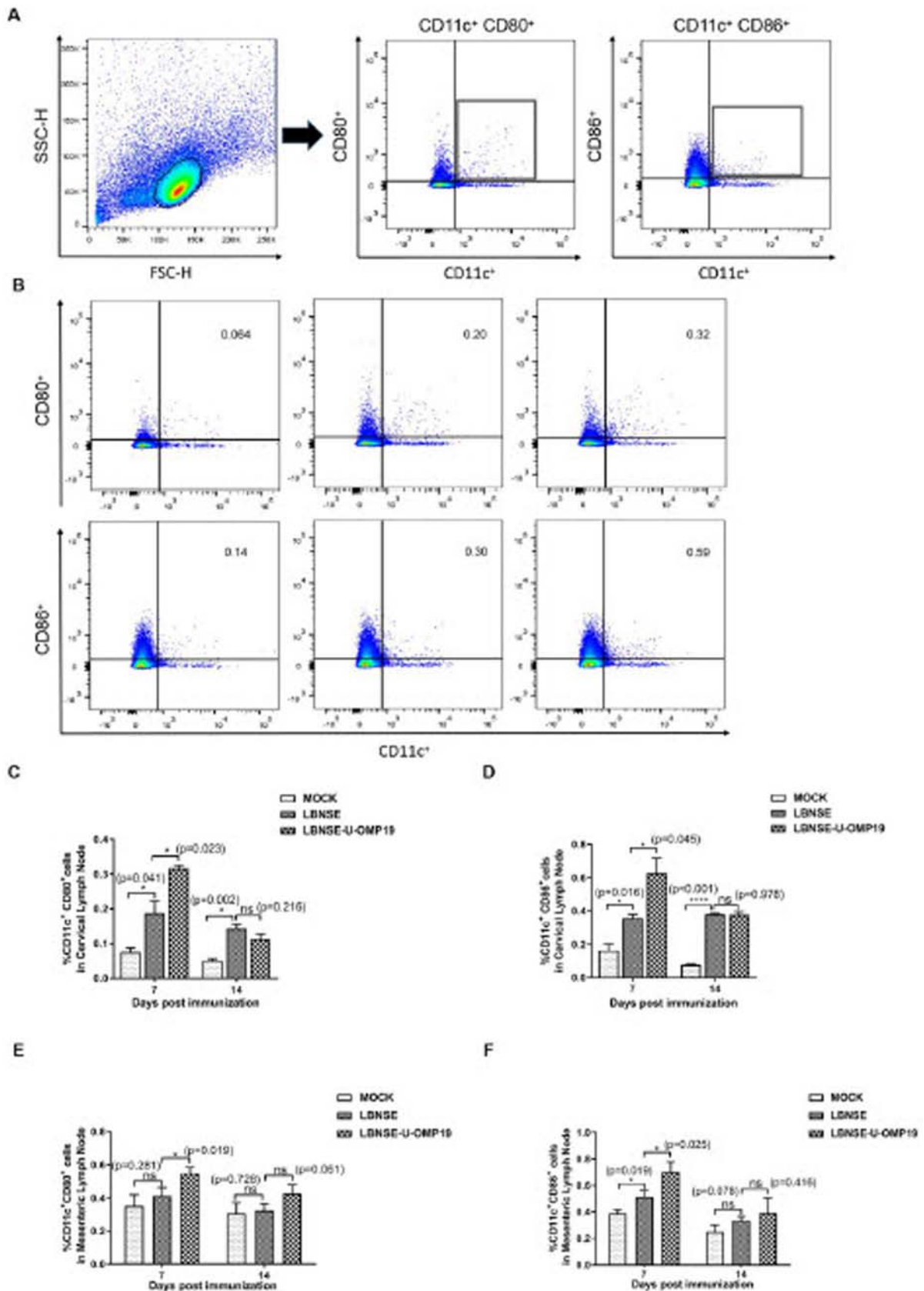


**Figure 3.** Recruitment and activation of DCs in orally immunized mice. Groups of six-week-old female ICR mice were orally immunized with  $10^7$  FFU of LBNSE or LBNSE-U-OMP19 or mock immunized with DMEM. CLNs and MLNs were harvested at 7 and 14 dpi. Single-cell suspensions prepared from collected lymph nodes were analysed for activated DCs by FACS. The gating strategies (A) and representative cytometric plots (B) for activated DCs ( $CD11c^+CD86^+$  or  $CD11c^+CD80^+$ ) are presented. The percentages of activated DCs ( $CD11c^+CD80^+$  or  $CD11c^+CD86^+$ ) in CLNs and MLNs (C–F) are shown. The data are representative of two independent experiments and are presented as the mean  $\pm$  SEM ( $n = 3$ ). (\* $p < 0.05$ ; ns: non-significant).



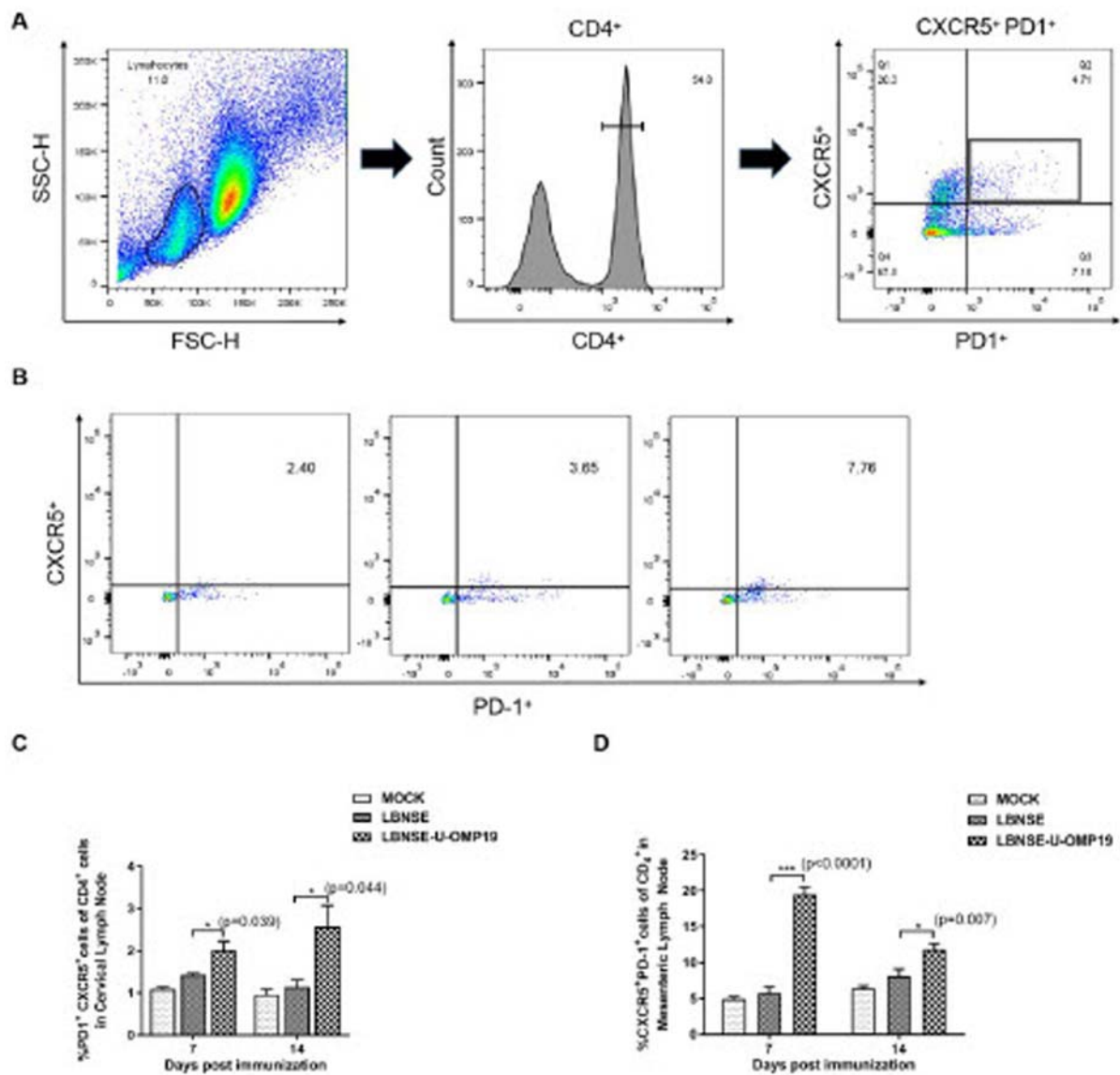


**Figure 4.** Recruitment of T<sub>FH</sub> cells in orally immunized mice. Groups of six-week-old female ICR mice were orally immunized with  $10^7$  FFU of LBNSE or LBNSE-U-OMP19 or mock immunized with DMEM. CLNs and MLNs were harvested at 7 and 14 dpi. Single-cell suspensions prepared from collected lymph nodes were analysed for the recruitment of T<sub>FH</sub> cells by FACS. The gating strategies (A) and representative cytometric plots (B) for T<sub>FH</sub> cells (CD4<sup>+</sup>CXCR5<sup>+</sup>PD-1<sup>+</sup>) are presented. The percentages of T<sub>FH</sub> cells detected in CLNs (C) and MLNs (D) in immunized mice are shown. The data are representative of two independent experiments and are presented as the mean  $\pm$  SEM ( $n = 3$ ). (\* $p < 0.05$ ; \*\*\* $p < 0.001$ ).

because of the interaction between T<sub>FH</sub> cells and B cells. Hence, T<sub>FH</sub> cells were detected in the CLNs and MLNs of orally immunized mice by FACS. The gating strategy and representative flow cytometric plots for T<sub>FH</sub> cells (PD1<sup>+</sup>CXCR5<sup>+</sup>CD4<sup>+</sup>) are shown in Figure 4(A) and (B), respectively. The numbers of T<sub>FH</sub> cells detected in both the CLNs and MLNs of mice immunized with LBNSE-U-OMP19 were significantly higher than those detected in the CLNs and MLNs of mice immunized with LBNSE at 7 and 14 dpi, as shown in Figure 4(C) and (D).

To investigate whether the expression of U-OMP19 by LBNSE-U-OMP19 can enhance the generation of GCs, the CLNs and MLNs of immunized mice were

harvested at 14 dpi, and the formation of GCs was measured via histology and immunofluorescence assays. Representative results for GC formation in the CLNs and MLNs of immunized mice at 14 dpi are shown in Figure 5(A) and (B), respectively, and significantly more GCs were observed in both the CLNs and MLNs of the mice immunized with LBNSE-U-OMP19 than in those immunized with LBNSE, as shown in Figure 5(C) and (D), respectively, as determined by calculating the numbers of GCs per CLN and MLN in immunized mice. These results indicate that the expression of U-OMP19 can enhance the recruitment of T<sub>FH</sub> cells and facilitate the formation of GCs in orally immunized mice.

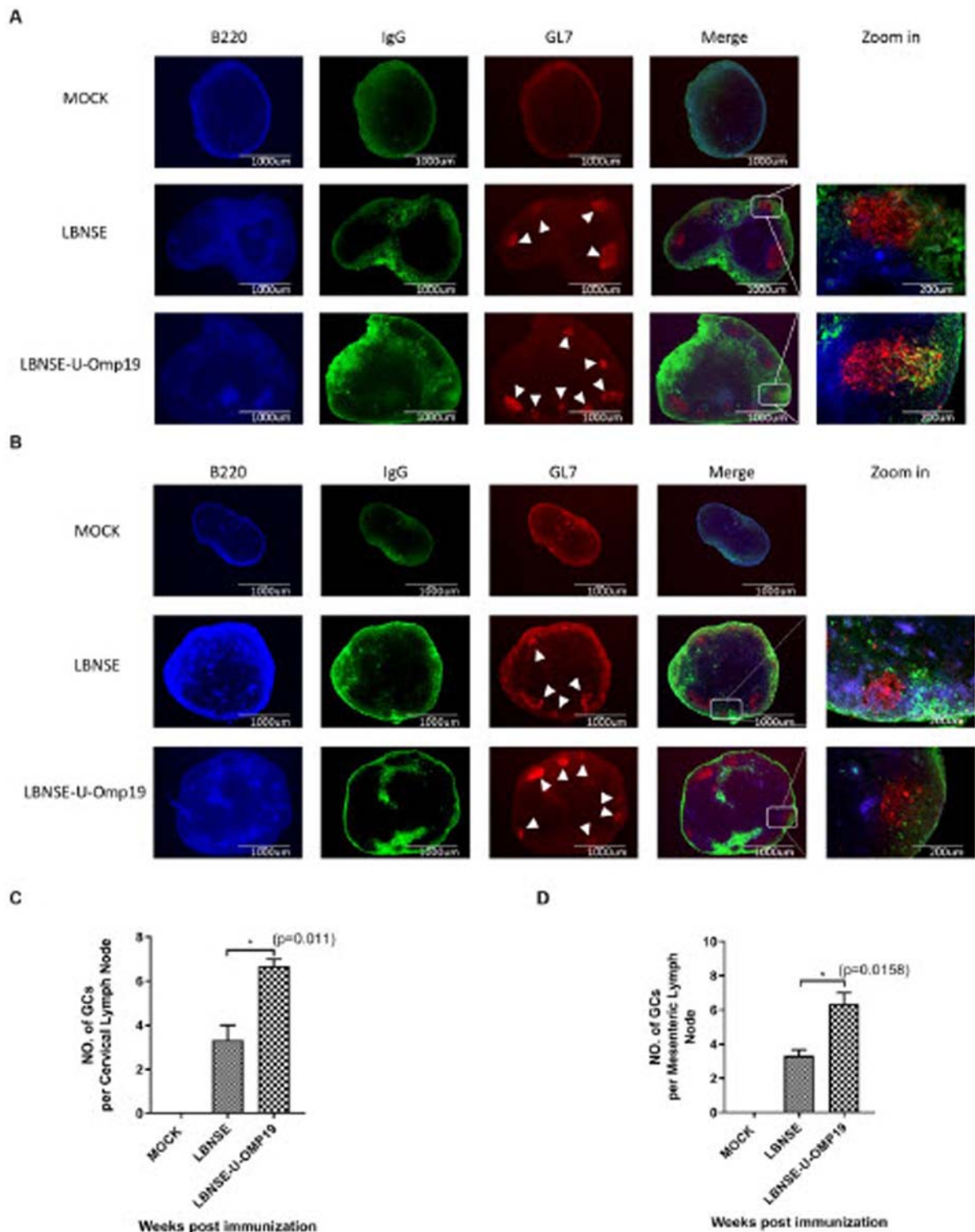


**Figure 5.** Generation of GCs in orally immunized mice. Groups of 6-week-old female ICR mice were orally immunized with  $10^7$  FFU of LBNSE or LBNSE-U-OMP19 or mock immunized with DMEM. CLNs and MLNs were harvested at 14 dpi. Tissue sections were prepared to detect GCs (B220<sup>+</sup>, blue; IgG<sup>+</sup>, green; GL7<sup>+</sup>, red). Scale bars, 1000 or 200  $\mu$ m (rightmost column only). The representative results of GC formation in CLNs (A) and MLNs (B) are shown. The numbers of GCs formed at 14 dpi in CLNs (C) and MLNs (D) were calculated. The data are representative of two independent experiments and are presented as the mean  $\pm$  SEM ( $n = 3$ ). (\* $p < 0.05$ ; \*\* $p < 0.01$ ).

#### **Expression of U-OMP19 augments GC B cell and PC populations in orally immunized mice**

Since T<sub>FH</sub> cells directly associate with GC B cells, the GC B cells (B220<sup>+</sup>CD95<sup>+</sup>GL7<sup>+</sup>) in CLNs and MLNs were quantified at 7 and 14 dpi. The gating strategy

and representative flow cytometric plots for GC B cells are shown in Figure 6(A) and (B), respectively. Significantly more GC B cells were detected in both CLNs and MLNs of the mice immunized with LBNSE-U-OMP19 than in those of mice immunized

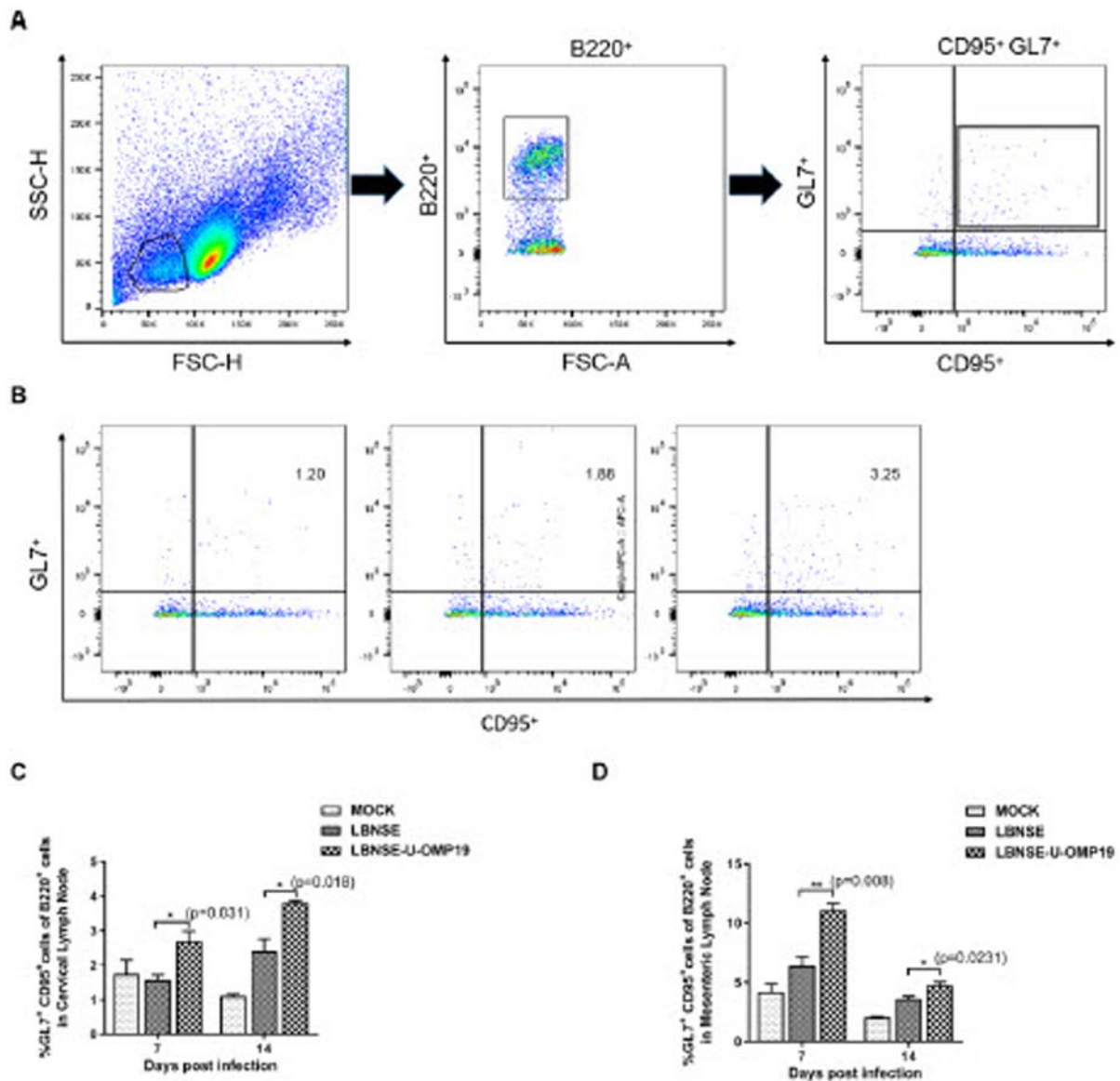


**Figure 6.** Generation of GC B cells in orally immunized mice. Groups of six-week-old female ICR mice were orally immunized with  $10^7$  FFU of LBNSE or LBNSE-U-OMP19 or mock immunized with DMEM. CLNs and MLNs were harvested at 7 and 14 dpi. Single-cell suspensions prepared from collected lymph nodes were analysed for GC B cells by FACS. The gating strategies (A) and representative cytometric plots (B) for GC B cells ( $B220^+CD95^+GL7^+$ ) are presented. The percentages of  $T_{FH}$  cells detected in CLNs (C) and MLNs (D) in immunized mice are shown. The data are representative of two independent experiments and are presented as the mean  $\pm$  SEM ( $n = 3$ ). (\* $p < 0.05$ ; \*\* $p < 0.01$ ).

with LBNSE, as shown in Figure 6(C) and (D), respectively.

GC B cells can further differentiate into PCs, which then leave secondary lymphoid organs to reside primarily in bone marrow for antibody production [35,36]. Hence, the generation of PCs in the bone marrow of immunized mice was also examined by FACS. The gate strategy and representative flow cytometric plots for PCs are shown in Figure 7(A) and (B), respectively. Significantly more PCs were detected in the bone marrow of the mice immunized with LBNSE-U-OMP19 than in those immunized with LBNSE at 14 dpi, as shown in Figure 7(C). These data indicate that the expression of U-OMP19 can increase the populations of GC B cells and PCs in orally immunized mice.

### Expression of U-OMP19 enhances VNA production and provides superior protection

To investigate whether the recruitment of activated DCs,  $T_{FH}$  cells, GC B cells and PCs and the increased generation of GCs can improve vaccine efficacy, groups of 20 ICR mice were orally immunized with  $10^7$  FFU of LBNSE-U-OMP19 or LBNSE or mock immunized with DMEM. Blood samples were collected weekly for five weeks to test for VNAs, and as shown in Figure 8(A), significantly higher levels of VNAs were detected in mice immunized with LBNSE-U-OMP19 than in those immunized with the parent virus LBNSE from 2 to 5 wpi. The average VNA titres of LBNSE immunized mice were 0.07, 0.40, 1.15, 0.85, and 0.64 IU/mL from 1 to 5 weeks post

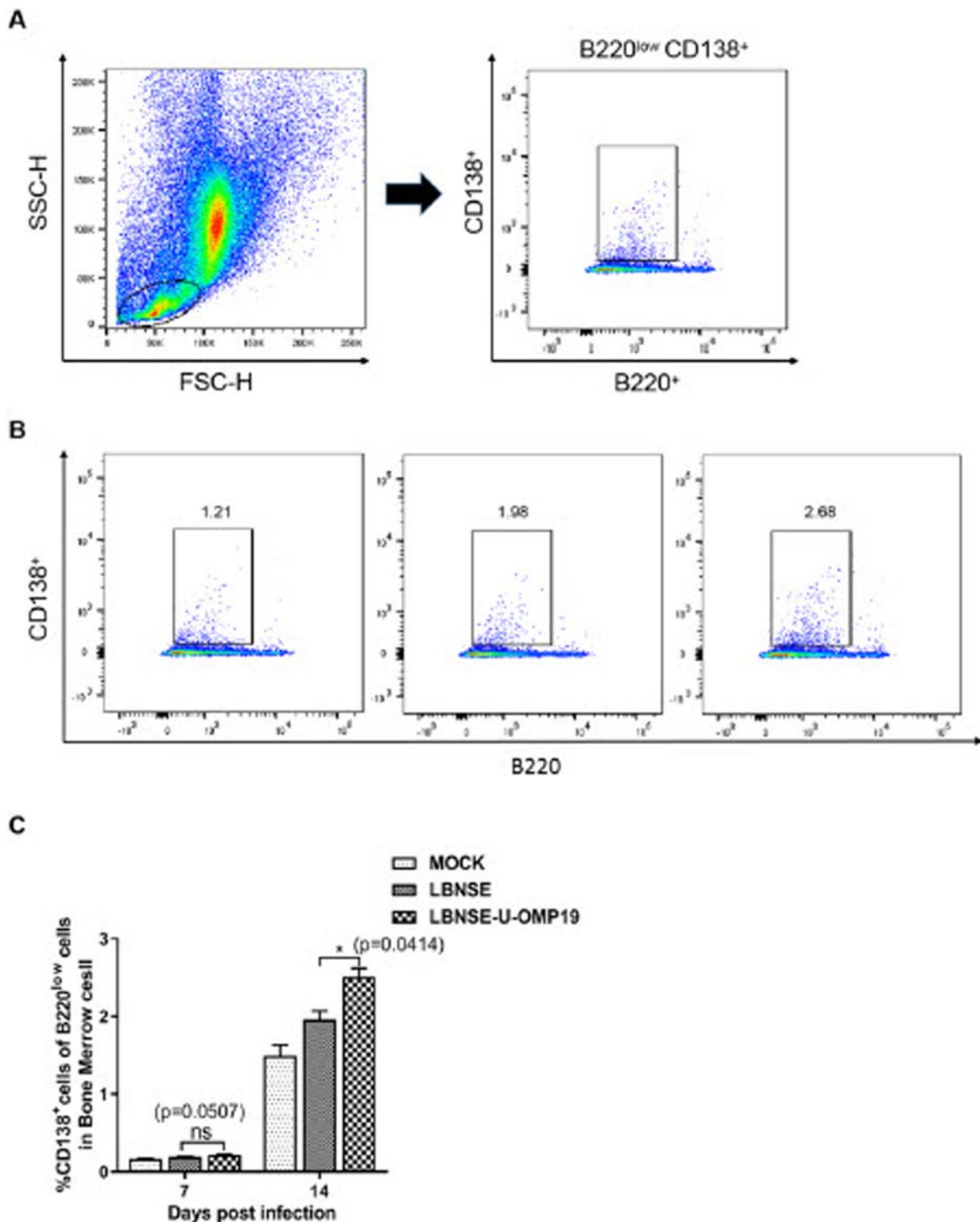


**Figure 7.** PCs populations in orally immunized mice. Groups of 6-week-old female ICR mice were orally immunized with  $10^7$  FFU of LBNSE or LBNSE-U-OMP19 or mock immunized with DMEM. Bone marrow was harvested at 7 and 14 dpi, and single-cell suspensions were prepared to detect PCs by FACS. The gating strategies (A) and representative cytometric plots (B) for PCs (B220<sup>low</sup>CD138<sup>+</sup>) are presented. The percentages of PCs detected in the bone marrow (C) of immunized mice are shown. The data are representative of two independent experiments and are presented as the mean  $\pm$  SEM ( $n = 3$ ). (\* $p < 0.05$ ; ns: non-significant).

immunization respectively, while the average VNA titres of LBNSE-U-OMP19 immunized mice were 0.34, 4.01, 6.98, 5.22, and 4.40 IU/mL from 1 to 5 weeks post immunization respectively. As for seroconversion of rabies vaccination, the VNA titre  $\geq 0.5$  IU/mL is considered to be protective [37]. According to the VNA titres of each immunized mice, the

seroconversion rates for LBNSE immunized mice were 0, 37.5%, 37.5%, 50% and 50% from 1 to 5 weeks post immunization respectively, while LBNSE-U-OMP19 immunized mice were 12.5%, 62.5%, 87.5%, 87.5% and 87.5% from 1 to 5 weeks post immunization respectively. In the literature, it has been reported that early vaccine-induced secretory IgM

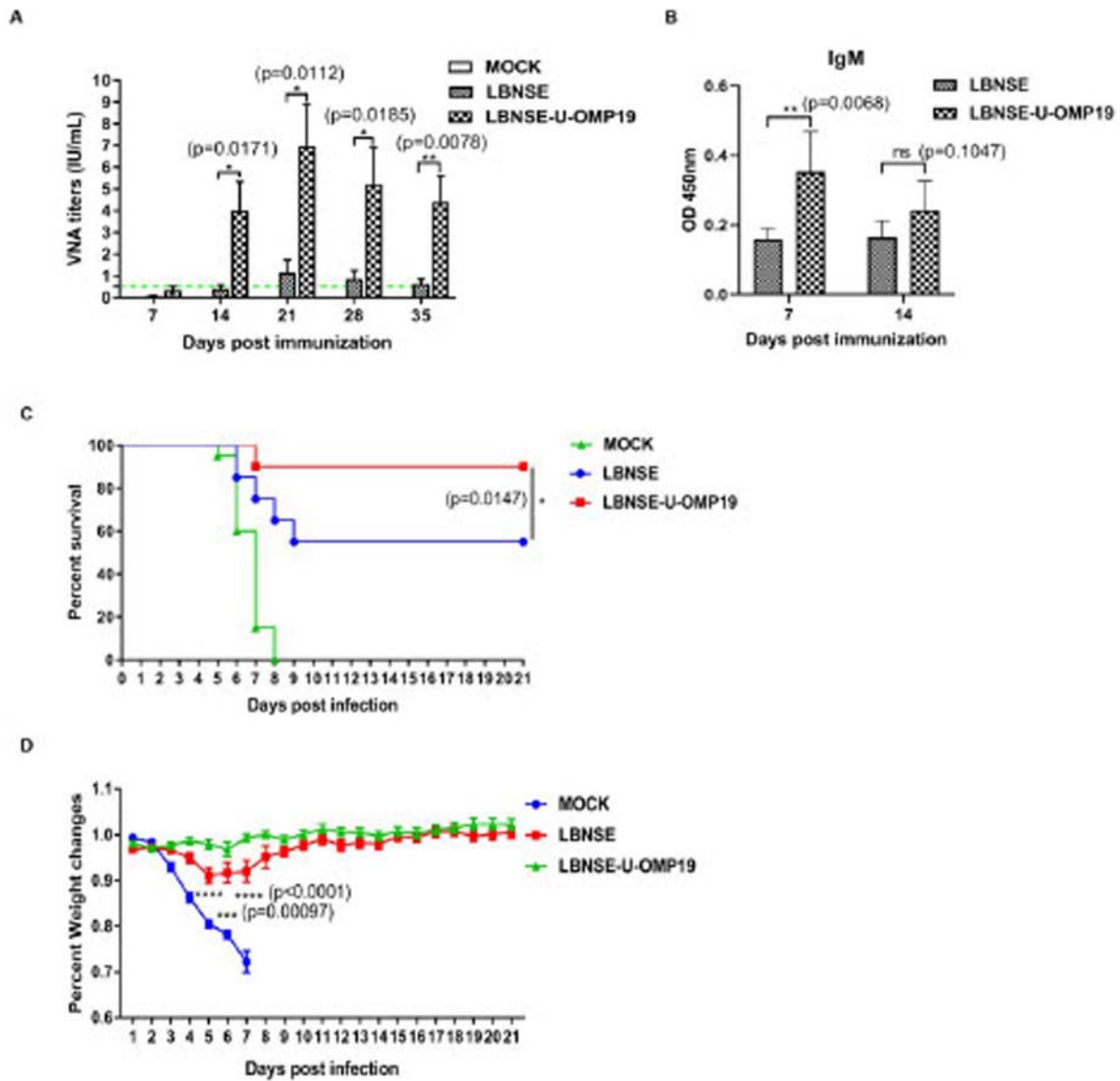


**Figure 8.** VNA production and protection after challenge of orally immunized mice. Groups of six-week-old female ICR mice ( $n = 10$ ) were orally immunized with  $10^7$  FFU of LBNSE or LBNSE-U-OMP19 or mock immunized with DMEM. At the indicated time points post immunization, peripheral blood samples were collected, sera were separated to quantify VNA titres by using FAVN (A), the green dash line indicates VNA titre of 0.5 IU/mL. The RABV-specific IgM antibody levels (B) in the collected sera samples were also measured by ELISA. The data are presented as the mean  $\pm$  SEM ( $n = 10$ ). To determine protection, groups of six-week-old female ICR mice ( $n = 20$ ) were orally immunized with  $10^7$  FFU of LBNSE or LBNSE-U-OMP19 or mock immunized with DMEM, and the immunized mice were infected via the i.c. route with 50 LD<sub>50</sub> of CVS-24 at 4 weeks post immunization, and the survival rates (C) and body weight changes (D) were monitored and recorded for 21 days. The data are representative of two independent experiments. (\* $p < 0.05$ ; \*\* $p < 0.01$ ; \*\*\* $p < 0.001$ ; \*\*\*\* $p < 0.0001$ ).

(SIgM) can limit the dissemination of pathogenic RABV to the CNS and mediate protection against pathogenic RABV challenge [38]. Therefore, blood samples of immunized mice were collected weekly for two weeks to measure the level of RABV-specific SIgM. As shown in Figure 8(B), significantly higher levels of SIgM were produced in LBNSE-U-OMP19-immunized mice than in LBNSE-immunized mice at 7 dpi. To further assess the vaccination efficacy, the immunized mice were challenged with 50 LD<sub>50</sub> of CVS-24 via the i.c. route. As expected, mice immunized with LBNSE-U-OMP19, mice immunized with

LBNSE and mice mock immunized with DMEM began to die of rabies at 8 dpi, from 6 to 9 dpi, or from 5 to 8 dpi, respectively. Ultimately, 90% of mice immunized with LBNSE-U-OMP19 were protected after challenge, while only 55% of LBNSE-immunized mice were protected, as shown in Figure 8(C). Moreover, the body weight changes of mice were also monitored after challenge as depicted in Figure 8(D), and significantly greater body weight changes after challenge were observed in LBNSE-immunized mice than in those immunized with LBNSE-U-OMP19 from 5 to 7 dpi. Overall, these

results show that expression of U-OMP19 by LBNSE-U-OMP19 can enhance VNA production and improve the survival rate of orally immunized mice.

Taken together, these data indicated that the expression of U-OMP19 can improve VNA production and protection by activating the DC- $T_{FH}$  cell-GC B cell-PC axis and generating more GCs in both CLNs and MLNs after oral immunization in mice, suggesting that LBNSE-U-OMP19 is a promising oral rabies vaccine strain.

## Discussion

Recent studies have indicated that oral immunization with U-OMP19 can induce the recruitment of DCs in the gut [26,31], and our previous studies have demonstrated that activation of DCs could improve the immunogenicity of rabies vaccines. Therefore, a recombinant RABV expressing U-OMP19 was constructed, and it was also found that DCs were recruited in LBNSE-U-OMP19-immunized mice. Moreover, the production of high-affinity antibodies by B cells is a hallmark of the humoral response, and activated B cells then undergo affinity maturation and differentiation in GCs after exposure to a specific antigen [39].  $T_{FH}$  cells regulate the size of GCs, limit the entry of low-affinity B cells into GCs, promote high-affinity B cell occupancy in GCs, and select high-affinity B cells during affinity maturation [40]. However, whether the formation of GCs can be induced by U-OMP19 remains unclear. In our study, we found that LBNSE-U-OMP19 enhanced the recruitment of  $T_{FH}$  cells and the formation of GCs in immunized mice. GCs are also the site of differentiation of long-lived memory B cells and long-lived PCs. The antibody-secreting PCs exported from GCs persist in bone marrow niches that support their longevity. As expected, more PCs were observed in the bone marrow of LBNSE-U-OMP19-immunized mice than in the bone marrow of LBNSE-immunized mice, which is consistent with the VNA titre results. These results indicate that U-OMP19 is a promising adjuvant for oral rabies vaccine that could enhance the immunogenicity by generating more GCs and activating DCs- $T_{FH}$ -GC B-PCs axis in orally immunized mice both in the oral cavity and gastrointestinal tract.

Besides efficacy, safety is an important factor for vaccine development [41]. Intriguingly, the expression of U-OMP19 attenuated RABV pathogenicity by restricting RABV transcription and replication in mouse brains. A previous study illustrated that lipided (L)-OMP16 and L-OMP19, but not their unlipided forms, induced inflammatory responses [42]. Similarly, decreased inflammatory chemokine or cytokine production was found in LBNSE-U-OMP19-injected mice, but the mechanism remains to be

further investigated in future studies. Additionally, to examine whether the vaccine virus would develop persistent infection in oral cavity and induce injury of lung and brains after oral vaccination, the viral RNA (vRNA) in buccal mucosa, CLN and tongues and the pathogenic injury of lungs and brains in immunized mice were detected by nest PCR and H&E staining analysis, respectively, as previous described [13,32]. As shown in Figure S4 and S5, no vRNA were detected in the tested samples, and no obvious injury were observed in lungs and brains of immunized mice after oral vaccination, respectively. All these data suggested that LBNSE-U-OMP19 is safe as an oral rabies vaccine [43]. Furthermore, regarding the safety of vaccines, killed oral vaccines could be a better choice than live vaccines. U-OMP19 was used as an adjuvant in oral killed vaccines in a previous study [31], and we confirmed that U-OMP19 can enhance the immunogenicity of an inactivated oral rabies vaccine (Figure S1).

Previous studies have demonstrated that replication of some viruses, such as HIV [44,45] and HCMV [46], can occur in gut-associated lymphoid tissue (GALT), where other viruses, including poliovirus [47] and dengue virus [48], replicate in Peyer's patches (PPs). In our study, however, the viral titres were not detectable after incubation with simulated gastric fluid, or relatively low after incubation with simulated intestinal fluid. Simultaneously, the viral RNA of vaccine virus was undetectable in buccal mucosa, CLN, and tongue at one and two days post oral immunization as shown in Figure S4. Therefore, we believe that LBNSE-U-OMP19 would be inactivated after travelling through the gastrointestinal tract after oral immunization. As it is known that the greatest barrier for oral vaccination lies in the gastrointestinal tract, which is a hostile environment and contains large quantities of proteases. In our study, we attempted to design a novel rabies vaccine with potential resist to those proteases in the gastrointestinal tract. We found that the recombinant virus LBNSE-U-OMP19 could potentially reduce the degradation of viral G protein and N protein after incubating with simulated gastrointestinal fluids (Figure 1(E) and (F)). However, the viral replication ability of LBNSE-U-OMP19 was dramatically decreased or even completely destroyed after incubation with simulated gastrointestinal fluids (Data not shown). Therefore, according to the results collected in our study so far, expression U-OMP19 by LBNSE-U-OMP19 could only possibly reduce the degradation of viral G protein *in vitro*, and whether this potential protection hold true *in vivo* still needs a further investigation.

The expression level of U-OMP19 could be crucial for the oral rabies vaccine efficacy, and there are several ways to improve the expression of U-OMP19 such as advancing the insertion position of the

U-OMP19 gene between the N and P genes or the P and M genes, as described previously [49]. Additionally, codon optimization or insertion of two or three copies of U-OMP19 could be potential options for improving this vaccine [50,51]. Furthermore, whether the incorporation of U-OMP19 into RABV virions would be more effective on reducing the degradation of viral antigens is worthy of investigation, which is warranted in our future study.

Together, our data suggest that LBNSE-U-OMP19 is a novel candidate for oral rabies vaccines that can enhance immunogenicity and improve protection after challenge by expressing U-OMP19 through activating the DC-T<sub>FH</sub> cell-GC B cell-PC axis. LBNSE-U-OMP19 has the potential to decrease the digestion of viral G protein by gastrointestinal proteases *in vitro*, and this will be further investigated *in vivo* in our future studies.

### Acknowledgements

The authors thank all the members of the Rabies group at HZAU.

### Disclosure statement

No potential conflict of interest was reported by the author(s).

### Funding

This study was partially supported by the National Key Research and Development Program of China [grant number: 2016YFD0500405 and 2017YFD0501701], the National Natural Science Foundation of China [grant number: 31872494, 31402176, 31372419 and 31522057], and the Natural Science Foundation of Hubei Province [grant number: 2019CFA010].

### Author contributions

The experiment was designed by MZ and LZ. The experiments were conducted by JZ, YZ, YC, JZ and JP. The data analysis was conducted by MZ, LZ, MC, and ZFF. The manuscript was drafted by JZ and YZ and revised by MZ and LZ.

### Ethics statement

The animal experiments were carried out in strict accordance with the protocols approved by The Scientific Ethics Committee of Huazhong Agricultural University (permit number: HZAUMO-2018-049). All institutional and national guidelines for the care and use of laboratory animals were followed.

### Data availability statement

All datasets generated for this study are included in the article.

### ORCID

Zhen F. Fu  <http://orcid.org/0000-0001-6293-9329>

### References

- [1] Fisher CR, Streicker DG, Schnell MJ. The spread and evolution of rabies virus: conquering new frontiers. *Nat Rev Microbiol.* 2018;16(4):241–255.
- [2] Fooks AR, Banyard AC, Horton DL, et al. Current status of rabies and prospects for elimination. *Lancet.* 2014;384(9951):1389–1399.
- [3] Hampson K, Coudeville L, Lembo T, et al. Estimating the global burden of endemic canine rabies. *PLoS Negl Trop Dis.* 2015;9(4):e0003709.
- [4] Vigilato MAN, Clavijo A, Knobl T, et al. Progress towards eliminating canine rabies: policies and perspectives from Latin America and the Caribbean. *Philos Trans Royal Soc London Ser B, Biol Sci.* 2013;368(1623):20120143–20120143.
- [5] Hu R, Tang Q, Tang J, et al. Rabies in China: an update. *Vector Borne Zoonotic Dis (Larchmont, NY).* 2009;9(1):1–12.
- [6] Abela-Ridder B. Rabies: 100 per cent fatal, 100 per cent preventable. *Vet Rec.* 2015;177(6):148–149.
- [7] Blackwood JC, Streicker DG, Altizer S, et al. Resolving the roles of immunity, pathogenesis, and immigration for rabies persistence in vampire bats. *Proc Natl Acad Sci USA.* 2013;110(51):20837–20842.
- [8] Tu C, Feng Y, Wang Y. Animal rabies in the People's Republic of China. *Rev Sci Tech.* 2018;37(2):519–528.
- [9] Campos AAS, Dos Santos RN, Benavides JA, et al. Rabies surveillance in wild mammals in South of Brazil. *Transbound Emerg Dis.* 2020;67(2):906–913.
- [10] Benavides JA, Megid J, Campos A, et al. Using surveillance of animal bite patients to decipher potential risks of rabies exposure from domestic animals and wildlife in Brazil. *Front Public Health.* 2020;8:318.
- [11] Health O W. WHO expert consultation on rabies. second report. *World Health Organ Tech Rep Ser.* 2013;982: 1–139.
- [12] Lafay F, Bénéjean J, Tuffereau C, et al. Vaccination against rabies: construction and characterization of SAG2, a double avirulent derivative of SADBern. *Vaccine.* 1994;12(4):317–320.
- [13] Orciari LA, Niezgodna M, Hanlon CA, et al. Rapid clearance of SAG-2 rabies virus from dogs after oral vaccination. *Vaccine.* 2001;19(31):4511–4518.
- [14] Cliquet F, Gurbuxani JP, Pradhan HK, et al. The safety and efficacy of the oral rabies vaccine SAG2 in Indian stray dogs. *Vaccine.* 2007;25(17):3409–3418.
- [15] Fekadu M, Nesby SL, Shaddock JH, et al. Immunogenicity, efficacy and safety of an oral rabies vaccine (SAG-2) in dogs. *Vaccine.* 1996;14(6):465–468.
- [16] Kieny MP, Lathe R, Drillien R, et al. Expression of rabies virus glycoprotein from a recombinant vaccinia virus. *Nature.* 1984;312(5990):163–166.
- [17] Robbins AH, Borden MD, Windmiller BS, et al. Prevention of the spread of rabies to wildlife by oral vaccination of raccoons in Massachusetts. *J Am Vet Med Assoc.* 1998;213(10):1407–1412.

- [18] Fearneyhough MG, Wilson PJ, Clark KA, et al. Results of an oral rabies vaccination program for coyotes. *J Am Vet Med Assoc.* 1998;212(4):498–502.
- [19] Stohr K, Meslin FM. Progress and setbacks in the oral immunisation of foxes against rabies in Europe. *Vet Rec.* 1996;139(2):32–35.
- [20] Centers for Disease Control and Prevention. Human vaccinia infection after contact with a raccoon rabies vaccine bait – Pennsylvania, 2009. *MMWR Morb Mortal Wkly Rep.* 2009;58(43):1204–1207.
- [21] Zhou M, Zhang G, Ren G, et al. Recombinant rabies viruses expressing GM-CSF or flagellin are effective vaccines for both intramuscular and oral immunizations. *PLoS One.* 2013;8(5):e63384.
- [22] Black JG, Lawson KF. Further studies of sylvatic rabies in the fox (*Vulpes vulpes*). vaccination by the oral route. *Can Vet J.* 1973;14(9):206–211.
- [23] Baer GM, Broderson JR, Yager PA. Determination of the site of oral rabies vaccination. *Am J Epidemiol.* 1975;101(2):160–164.
- [24] Pasquevich KA, Estein SM, García Samartino C, et al. Immunization with recombinant *Brucella* species outer membrane protein Omp16 or Omp19 in adjuvant induces specific CD4+ and CD8+ T cells as well as systemic and oral protection against *Brucella abortus* infection. *Infect Immun.* 2009;77(1):436–445.
- [25] Coria LM, Risso GS, Guaimas FF, et al. Oral co-administration of a bacterial protease inhibitor in the vaccine formulation increases antigen delivery at the intestinal epithelial barrier. *J Control Release.* 2019;293:158–171.
- [26] Ibanez AE, Coria LM, Carabajal MV, et al. A bacterial protease inhibitor protects antigens delivered in oral vaccines from digestion while triggering specific mucosal immune responses. *J Control Release.* 2015;220(Pt A):18–28.
- [27] Faber M, Faber ML, Papaneri A, et al. A single amino acid change in rabies virus glycoprotein increases virus spread and enhances virus pathogenicity. *J Virol.* 2005;79(22):14141–14148.
- [28] Wen Y, Wang H, Wu H, et al. Rabies virus expressing dendritic cell-activating molecules enhances the innate and adaptive immune response to vaccination. *J Virol.* 2011;85(4):1634–1644.
- [29] Inoue K, Shoji Y, Kurane I, et al. An improved method for recovering rabies virus from cloned cDNA. *J Virol Methods.* 2003;107(2):229–236.
- [30] Zhao L, Toriumi H, Kuang Y, et al. The roles of chemokines in rabies virus infection: overexpression may not always be beneficial. *J Virol.* 2009;83(22):11808–11818.
- [31] Risso GS, Carabajal MV, Bruno LA, et al. U-Omp19 from *Brucella abortus* is a useful adjuvant for vaccine formulations against *Salmonella* infection in mice. *Front Immunol.* 2017;8:171.
- [32] Zhou M, Wang L, Zhou S, et al. Recombinant rabies virus expressing dog GM-CSF is an efficacious oral rabies vaccine for dogs. *Oncotarget.* 2015;6(36):38504–38516.
- [33] Cliquet F, Aubert M, Sagné L. Development of a fluorescent antibody virus neutralisation test (FAVN test) for the quantitation of rabies-neutralising antibody. *J Immunol Methods.* 1998;212(1):79–87.
- [34] Wang Z, Li M, Zhou M, et al. A novel rabies vaccine expressing CXCL13 enhances humoral immunity by recruiting both T follicular helper and germinal center B cells. *J Virol.* 2017;91(3).
- [35] Hargreaves DC, Hyman PL, Lu TT, et al. A coordinated change in chemokine responsiveness guides plasma cell movements. *J Exp Med.* 2001;194(1):45–56.
- [36] Tokoyoda K, Hauser AE, Nakayama T, et al. Organization of immunological memory by bone marrow stroma. *Nat Rev Immunol.* 2010;10(3):193–200.
- [37] Monaco F, Franchi P, Lelli R. Studies on an inactivated vaccine against rabies virus in domestic animals. *Dev Biol (Basel).* 2006;125:233–239.
- [38] Dorfmeier CL, Shen S, Tzvetkov EP, et al. Reinvestigating the role of IgM in rabies virus postexposure vaccination. *J Virol.* 2013;87(16):9217–9222.
- [39] Bartlett BL, Pellicane AJ, Tyring SK. Vaccine immunology. *Dermatol Ther.* 2009;22(2):104–109.
- [40] Crotty S. T follicular helper cell differentiation, function, and roles in disease. *Immunity.* 2014;41(4):529–542.
- [41] Hsu A, Tseng C, Barrat J, et al. Safety, efficacy and immunogenicity evaluation of the SAG2 oral rabies vaccine in Formosan ferret badgers. *PloS One.* 2017;12(10):e0184831.
- [42] Giambartolomei GH, Zwerdling A, Cassataro J, et al. Lipoproteins, not lipopolysaccharide, are the key mediators of the proinflammatory response elicited by heat-killed *Brucella abortus*. *J Immunol.* 2004;173(7):4635–4642.
- [43] Mähl P, Cliquet F, Guiot A, et al. Twenty year experience of the oral rabies vaccine SAG2 in wildlife: a global review. *Vet Res.* 2014;45(77).
- [44] Guadalupe M, Sankaran S, George MD, et al. Viral suppression and immune restoration in the gastrointestinal mucosa of human immunodeficiency virus type 1-infected patients initiating therapy during primary or chronic infection. *J Virol.* 2006;80(16):8236–8247.
- [45] Chun TW, Nickle DC, Justement JS, et al. Persistence of HIV in gut-associated lymphoid tissue despite long-term antiretroviral therapy. *J Infect Dis.* 2008;197(5):714–720.
- [46] Sinzger C, Grefte A, Plachter B, et al. Fibroblasts, epithelial cells, endothelial cells and smooth muscle cells are major targets of human cytomegalovirus infection in lung and gastrointestinal tissues. *J Gen Virol.* 1995;76(Pt 4):741–750.
- [47] Shen L, Chen CY, Huang D, et al. Pathogenic events in a nonhuman primate model of oral poliovirus infection leading to paralytic poliomyelitis. *J Virol.* 2017;91(14).
- [48] Prestwood TR, May MM, Plummer EM, et al. Trafficking and replication patterns reveal splenic macrophages as major targets of dengue virus in mice. *J Virol.* 2012;86(22):12138–12147.
- [49] Mebatsion T, Schnell MJ, Cox JH, et al. Highly stable expression of a foreign gene from rabies virus vectors. *Proc Natl Acad Sci U S A.* 1996;93(14):7310–7314.
- [50] Pei J, Huang F, Wu Q, et al. Codon optimization of G protein enhances rabies virus-induced humoral immunity. *J Gen Virol.* 2019;100(8):1222–1233.
- [51] Li J, Ertel A, Portocarrero C, et al. Postexposure treatment with the live-attenuated rabies virus (RV) vaccine TriGAS triggers the clearance of wild-type RV from the central nervous system (CNS) through the rapid induction of genes relevant to adaptive immunity in CNS tissues. *J Virol.* 2012;86(6):3200–3210.